

Complex magnetic ordering in $\text{Tb}_3\text{Ag}_4\text{Sn}_4$

Laura K. Perry^{a)} and D. H. Ryan

Centre for the Physics of Materials, McGill University, Montréal, Québec H3A 2T8, Canada
and Physics Department, McGill University, Montréal, Québec H3A 2T8, Canada

F. Canepa and M. Napoletano

Dipartimento di Chimica e Chimica Industriale, Università degli Studi di Genova, Via Dodecaneso 31, 16146 Genova, Italy

D. Mazzone and P. Riani

INSTM, Via G. Giusti 9, 50121 Firenze, Italy and Dipartimento di Chimica e Chimica Industriale, Università degli Studi di Genova, Via Dodecaneso 31, 16146 Genova, Italy

J. M. Cadogan

School of Physics, The University of New South Wales, Sydney, New South Wales 2052, Australia

(Presented on 1 November 2005; published online 18 April 2006)

$\text{Tb}_3\text{Ag}_4\text{Sn}_4$ has been studied using both bulk magnetization and ^{119}Sn Mössbauer spectroscopy. We find evidence for a first-order magnetostructural transition at 28 K, followed by a spin reorientation at 13 K. Three tin sites with hyperfine fields of 8.0, 4.2, and 3.5 T are observed at 2 K with area ratios of 2:1:1. Magnetization at 5 K is linear up to 9 T, indicating antiferromagnetic ordering.

© 2006 American Institute of Physics. [DOI: 10.1063/1.2162826]

I. INTRODUCTION

The orthorhombic $R_3T_4X_4$ family (where R is a rare earth, $T=\text{Cu, Ag, Au}$, and $X=\text{Si, Ge, Sn}$) represents an extensive series of isostructural compounds that exhibit a rich variety of magnetic ordering. They crystallize in an orthorhombic $\text{Gd}_3\text{Cu}_4\text{Ge}_4$ -type structure (space group $Immm$, No. 71).¹ The rare-earth atoms occupy two crystallographically distinct sites ($4e$ and $2d$) and their moments order antiferromagnetically (AF), often with quite different moment values^{2,3} and with distinct magnetic structures adopted by the two rare-earth sublattices. In some cases the two rare-earth sites will also have two quite different ordering temperatures.⁴

As part of our on-going study of this complex alloy system, we turn to the compound $\text{Tb}_3\text{Ag}_4\text{Sn}_4$. We present here the results of bulk characterization by susceptibility and magnetization, complemented by a microscopic investigation of the ordering using ^{119}Sn Mössbauer spectroscopy. We find two magnetic ordering transitions, with evidence for the upper one being a first-order event, possibly involving a change in crystal structure.

II. EXPERIMENTAL METHODS

A stoichiometric quantity of the pure elements (99.9 wt. % Tb and 99.999 wt. % Ag and Sn) was induction melted in a sealed tantalum crucible under high-purity argon. The alloy button was then sealed under vacuum in quartz tubes and annealed for 20 days at 873 K followed by water quenching. Cu $K\alpha$ x-ray-diffraction and electron microprobe analyses confirmed that the majority phase was the orthorhombic $\text{Tb}_3\text{Ag}_4\text{Sn}_4$ alloy, with less than 5% of the ζ -phase $\text{Ag}_{79}\text{Sn}_{21}$. Fitting of the diffraction patterns using GSAS (Ref.

5)/EXPGUI (Ref. 6), gave lattice parameters of $a=15.1581(4)$ Å, $b=7.3034(17)$ Å, and $c=4.5502(11)$ Å, consistent with other isostructural $R_3\text{Ag}_4\text{Sn}_4$ alloys.^{7,8} Basic magnetic characterization was carried out on a commercial susceptometer/magnetometer. ^{119}Sn transmission Mössbauer spectra were collected on a constant acceleration spectrometer using a 0.4 GBq ^{119m}Sn CaSnO_3 source with the sample in a helium flow cryostat. The spectrometer was calibrated using ^{57}Co and $\alpha\text{-Fe}$. Spectra were fitted using a conventional nonlinear least-squares minimization routine.

III. RESULTS AND DISCUSSION

The temperature dependence of the ac susceptibility, $\chi_{ac}(T)$, of $\text{Tb}_3\text{Ag}_4\text{Sn}_4$ in a drive field of 1 mT at 137 Hz (Fig. 1) clearly shows evidence of two magnetic transitions at 13 and 28 K. However, $\chi_{ac}(T)$ measured in the presence of a 1 T dc bias field shows only the lower transition at 13 K, the 28 K event being suppressed. Fitting the high-temperature

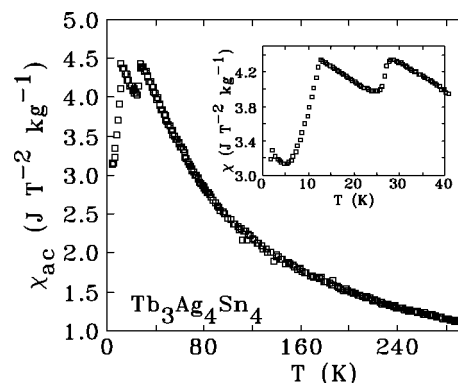
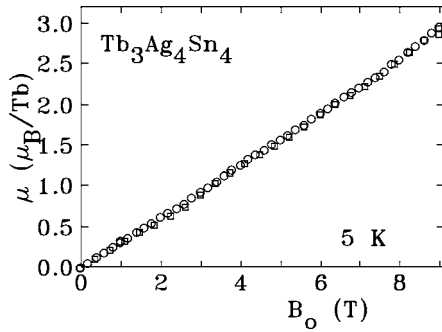


FIG. 1. ac susceptibility (χ_{ac}) as a function of temperature for $\text{Tb}_3\text{Ag}_4\text{Sn}_4$. Inset shows region below 40 K in more detail. Two magnetic transitions at 13 and 28 K are apparent.

^{a)}Electronic mail: perryll@physics.mcgill.ca

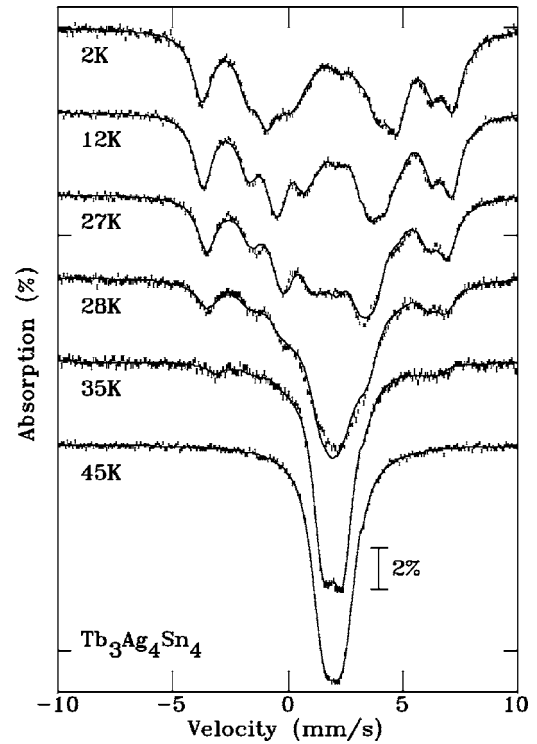
FIG. 2. Magnetization vs field for $\text{Tb}_3\text{Ag}_4\text{Sn}_4$ at 5 K.

region (150–300 K) of $\chi_{\text{ac}}(T)$ to a Curie-Weiss law yields $\theta_{\text{CW}} = -11$ K, confirming that the dominant exchange interactions are antiferromagnetic. The fit also yields an effective moment of $9.90(5) \mu_B/\text{Tb}$, close to the expected $9.72 \mu_B/\text{Tb}$. The linear field dependence of the magnetization at 5 K (Fig. 2) is consistent with AF ordering of the Tb moments and remains well below saturation in our maximum field of 9 T.

^{119}Sn Mössbauer spectroscopy provides an ideal window onto the magnetic ordering in these complex $R_3T_4\text{Sn}_4$ alloys. Tin has no magnetic moment, so that any hyperfine field (B_{hf}) observed in a ^{119}Sn Mössbauer spectrum must be due to ordered moments on neighboring sites. The tin atoms in $R_3T_4\text{Sn}_4$ occupy two crystallographic sites ($4f$ and $4h$) and both tin sites have neighbors from each of the two rare-earth sites in the structure.⁴ As a result, changes in magnetic ordering at either rare-earth site will affect B_{hf} at both tin sites.

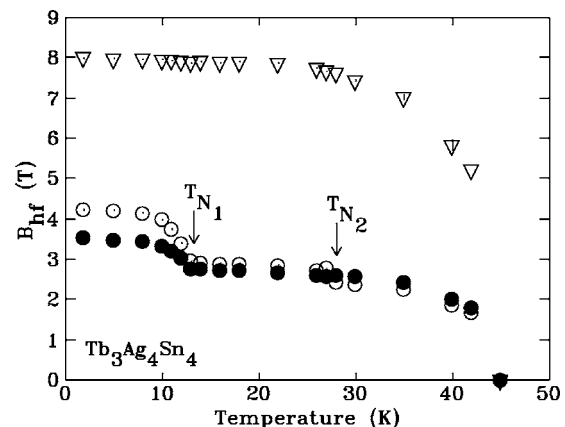
At 45 K, the alloy is paramagnetic and the ^{119}Sn Mössbauer spectrum consists of two unresolved equal-area quadrupole doublets, consistent with the crystal structure. At 2 K, well below both ordering transitions seen in the susceptibility, the spectrum is well split, showing significant hyperfine fields (see Fig. 3). Analysis of this 2 K spectrum, however, reveals a significant contradiction: It does not consist of the two equal-area magnetic sextets demanded by the crystal structure. The more widely split sextet with $B_{\text{hf}} = 8.00(1)$ T (which we will label Sn_A) does account for half of the total area, but the remaining contribution cannot be fitted with a single sextet without invoking an unrealistic linewidth, and even then a severe misfit is observed. Dividing the second, lower field component further into two equal halves (Sn_{B_1} with $B_{\text{hf}} = 4.22(3)$ T and Sn_{B_2} with $B_{\text{hf}} = 3.53(3)$ T) gives a far better fit and also permits a common linewidth to be used for all three components at all temperatures. However, the 2:1:1 area ratio observed in the fit to the 2 K Mössbauer spectrum is not immediately consistent with the constraints imposed by the room-temperature crystal structure.

The temperature dependence of B_{hf} at the Sn_{B_1} and Sn_{B_2} sites clearly shows the effects of the lower transition, T_{N_1} , at 13.5(5) K (Fig. 4). However, essentially no change in B_{hf} is seen at the Sn_A site. We also find that the electric-field gradient (efg) at the Sn_B sites undergoes a marked change at T_{N_1} . Since we are using a first-order perturbation expansion in the fitting, we are sensitive only to the projection of the efg onto the magnetic-field direction through

FIG. 3. ^{119}Sn Mössbauer spectra of $\text{Tb}_3\text{Ag}_4\text{Sn}_4$. Solid lines are fits described in the text.

$$\text{efg} \propto V_{zz}(3 \cos^2 \theta - 1),$$

where V_{zz} is the principal component of the efg tensor and θ is the angle between V_{zz} and B_{hf} (an axially symmetric efg is assumed here). It is unlikely that a crystallographic distortion large enough to cause the observed changes in the efg at the two Sn_B sites would not also affect the Sn_A site; therefore it is more probable that the change occurs in θ , i.e., the angle between V_{zz} and B_{hf} . A change in the orientation of B_{hf} relative to V_{zz} combined with a reduction in the size of B_{hf} could be caused by a loss of magnetic order at one of the two Tb sites, making $\text{Tb}_3\text{Ag}_4\text{Sn}_4$ similar to the $\text{Er}_3\text{Cu}_4\text{X}_4$ system where the two Er sites have quite different ordering temperatures.²⁻⁴ Alternatively, the change could be due to a

FIG. 4. Temperature dependence of the hyperfine fields (B_{hf}) at the three sites in $\text{Tb}_3\text{Ag}_4\text{Sn}_4$ showing the two magnetic transitions at T_{N_1} and T_{N_2} . \circ and \bullet show the fields for the Sn_{B_1} and Sn_{B_2} sites (areas=1:1), while ∇ shows B_{hf} at the Sn_A site (area=2). See text for details.

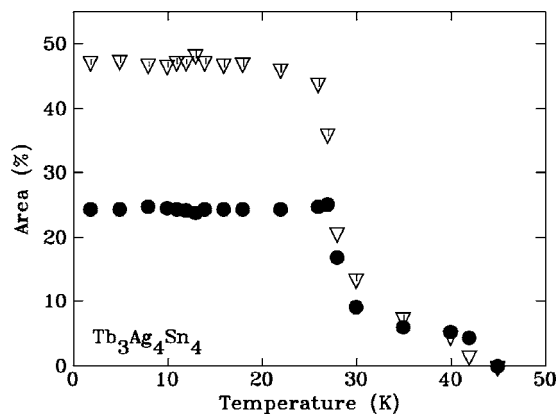


FIG. 5. Temperature dependence of the areas of the three components in the ^{119}Sn Mössbauer spectra of $\text{Tb}_3\text{Ag}_4\text{Sn}_4$ showing a transition at ~ 28 K. \circ and \bullet show the Sn_{B_1} and Sn_{B_2} sites, while ∇ shows the Sn_A site.

rotation of the magnetic ordering direction at one of the two Tb sites (a change at both Tb sites would almost certainly affect the high-field site as well, as both crystallographic tin sites have first-neighbor terbium atoms from both crystallographic Tb sites), making T_{N_1} a spin reorientation transition rather than a distinct ordering temperature. The ^{119}Sn Mössbauer data do not permit us to distinguish these two cases without additional information.

χ_{ac} in Fig. 1 clearly places the second transition at 28 K, but it is equally clear from Fig. 4 that little, if anything, happens in $B_{\text{hf}}(T)$ at any of the tin sites. Indeed, extrapolation of $B_{\text{hf}}(T)$ for all three tin sites leads to a common transition temperature of 44(1) K, where $\chi_{ac}(T)$ is essentially featureless. Closer examination of the spectra in Fig. 3 shows that $B_{\text{hf}}(T)$ does not tell the whole story. The line near -4 mm/s is a prominent feature of the 2 K spectrum and is the left-most line of the sextet due to the Sn_A site. With increasing temperature, this line moves to a slightly more positive velocity as B_{hf} falls; however, it also decreases markedly in intensity (compare the 28 and 35 K spectra in Fig. 3). Similar behavior is also observed at the Sn_{B_1} and Sn_{B_2} sites, although their splittings are much smaller and the changes are largely masked by the growth of the central paramagnetic components. The fitted area changes are shown in Fig. 5 and this confirms that it is the collapse of the area of the magnetic components that corresponds to T_{N_2} in χ_{ac} and not the collapse of the field as would be expected for a second-order magnetic transition.

The temperature dependences of B_{hf} (Fig. 4) and spectral areas (Fig. 5) are precisely those that would be expected for a first-order magnetostructural transition as is seen in the R_5X_4 giant magnetocaloric materials.^{9,10} The bulk of the transformation occurs between 24 and 30 K and it would appear that the upper feature in $\chi(T)$ (Fig. 1) seen at ~ 28 K corresponds to the steepest decline in magnetic area in Fig. 5 at 27.5(5) K. Remarkably, enough of the low-temperature phase persists at temperatures above which most of the material has transformed into the high-temperature form, and this allows us to estimate an ordering temperature of 44(1) K for the low-temperature form. However, we see no indications of magnetic order in the high-temperature form as it transforms before any magnetic order can develop.

Our measurements suggest that $\text{Tb}_3\text{Ag}_4\text{Sn}_4$ undergoes a first-order magnetostructural transition at 28 K, followed by a spin reorientation at 13 K. A change in crystal structure at 28 K is also consistent with the observed 2:1:1 area ratios for the $\text{Sn}_A:\text{Sn}_{B_1}:\text{Sn}_{B_2}$ sites in the 2 K ^{119}Sn Mössbauer spectrum. A neutron-diffraction study is underway to investigate this system in more detail.

ACKNOWLEDGMENTS

This work was supported by grants from the Natural Sciences and Engineering Research Council of Canada, Fonds pour la formation de chercheurs et l'aide à la recherche, Québec, and the Australian Research Council.

- ¹W. Rieger, *Monatsch. Chem.* **101**, 449 (1970).
- ²E. Wawrzyńska, J. Hernandez-Velasco, B. Penc, W. Sikora, A. Szytuła, and A. Zygunt, *J. Phys.: Condens. Matter* **15**, 5279 (2003).
- ³E. Wawrzyńska, J. Hernandez-Velasco, B. Penc, A. Szytuła, and A. Zygunt, *J. Magn. Magn. Mater.* **264**, 192 (2003).
- ⁴D. H. Ryan, J. M. Cadogan, R. Gagnon, and I. P. Swainson, *J. Phys.: Condens. Matter* **16**, 3183 (2004).
- ⁵A. C. Larson and R. B. Von Dreele, "General Structure Analysis System (GSAS)," Los Alamos National Laboratory Report No. LAUR 86-748, 2000; www.ncnr.nist.gov/programs/crystallography/software/gsas.html
- ⁶B. H. Toby, *J. Appl. Crystallogr.* **34**, 210 (2001).
- ⁷E. Wawrzyńska, J. Hernandez-Velasco, B. Penc, A. Szytuła, and K. Tomala, *J. Phys.: Condens. Matter* **16**, 7535 (2004).
- ⁸D. Mazzone, P. Riani, M. Napoletano, and F. Canepa, *J. Alloys Compd.* **387**, 15 (2005).
- ⁹K. A. Gschneidner, V. K. Pecharsky, A. O. Pecharsky, V. V. Ivchenko, and E. M. Levin, *J. Alloys Compd.* **303–304**, 214 (2000).
- ¹⁰D. H. Ryan, M. Elouneq-Jamroz, J. van Lierop, Z. Altounian, and H. B. Wang, *Phys. Rev. Lett.* **90**, 117202 (2003).